Structural Engineering and Mechanics, *Vol. 65, No. 1 (2018) 99-110*
DOI: https://doi.org/10.12989/sem.2018.65.1.099

Two new triangular finite elements containing stable open cracks

Mohammad Rezaiee-Pajand* and Nima Gharaei-Moghaddam[a]

Department of Civil Engineering, School of Engineering, Ferdowsi University of Mashhad, Iran

(Received July 10, 2017, Revised September 14, 2017, Accepted September 18, 2017)

Abstract. The focus of this paper is on the elements with stable open cracks. To analyze plane problems, two triangular elements with three and six nodes are formulated using force method. Flexibility matrices of the elements are derived by combining the non-cracked flexibility and the additional one due to crack, which is computed by utilizing the local flexibility method. In order to compute the flexibility matrix of the intact element, a basic coordinate system without rigid body motions is required. In this paper, the basic system origin is located at the crack center and one of its axis coincides with the crack surfaces. This selection makes it possible to formulate elements with inclined cracks. It is obvious that the ability of the suggested elements in calculating accurate natural frequencies for cracked structures, make them applicable for vibration-based crack detection.

Keywords: triangular cracked element; released strain energy; fracture mechanics; stress intensity factor; local flexibility approach

1. Introduction

Engineering structures sustain various damages during their service lifespan. Among these damages, internal cracks, which their initiation and propagation decrease the structural strength considerably, are more common. Therefore, crack detection and analysis of the cracked structures are very essential topics in structural engineering investigations. Various approaches such as the finite element method (FEM) (Formica and Milicchio 2016, Ma and Kwan 2016, Millwater *et al*. 2016), smoothed finite elements (Bordas *et al*. 2010, Nquyen-Xuan *et al*. 2012, Nguyen-zuan *et al*. 2013), the boundary element method (Aliabadi and Rooke 2002, Mi and Aliabadi 1992), meshless techniques (Belytschko *et al*. 1995, Duflot and Nxuyen-Xuan 2004) and extended finite element (Dolbow *et al*. 1999, Ventura *et al*. 2009) are applied to model and analyze the cracked structures. Recently, the newly introduced isogeometric method has been also applied for fracture mechanic's analysis (Verhoosel *et al*. 2011). Among these methods, finite element is used more frequently because of its inherent advantages and capabilities. However, the FEM can be used directly to evaluate cracked structures, but it faces some drawbacks. The main difficulty is to compute singularity of the stresses at the crack tips. This is caused by the convenient finite elements which take advantage of simple polynomial functions for interpolating displacement, stress and strain fields. To capture enough accurate responses, special shape functions or superior evaluation methods are necessary. If only common finite elements are available, a fine mesh in the location of the crack tip is required to reach an acceptable precision. It is obvious that this technique would decrease efficiency of the analysis remarkably.

In the early 1970, it was realized that the convenient finite elements provide poor accuracy in analysis of cracked structures. Therefore, special finite elements are proposed for fracture mechanic applications. A group of these elements take advantage of specific singular shape functions and are called “Crack Tip Elements” or simply CTE. CTEs are only used to discretize around the cracks, while the rest of structure is modeled using common elements. One of the main difficulties in utilizing CTEs is that their singular shape functions are incompatible with the convenient elements. In addition, most of these new elements are not introduced to the available finite element programs. The greatest advancement in this field was the formulation of the first quarter-point elements (QPE) by Henshell and Shaw (1975) and Barsoum (1976). The main idea behind the QPE formulation is to shift the coordinate of the mid-side nodes of an isoparametric element to quarter-point position in the direction of the crack tips for all elements' edges, which points to the crack tip. This position alteration leads to change in displacement, stress and strain field such that they demonstrate the desired singular behavior. Many investigators utilized this method and proposed various 2D and 3D finite elements (Banks-Sills and Bortman 1984, Hussain *et al*. 1981, Manu 1983, Banks-Sills and Sherman 1989, Alwar and Nambissan 1983).

Another group of CTEs are hybrid elements, which take advantage of analytical solutions in the element formulation, and their boundary conditions are selected such that makes them compatible with other isoparametric elements. To derive fracture parameters, such as stress intensity factors, using these elements, no interpolation or

*Corresponding author, Professor
E-mail: Rezaiee@um.ac.ir
[a]Ph.D. Student
E-mail: Nima.Gharaei@gmail.com

ISSN: 1225-4568 (Print), 1598-6217 (Online)

additional effort is needed. This is attributable to the application of the fracture parameters in the element formulation directly. The only drawback of these elements is the difficulty in their formulation. The first hybrid crack tip element presented by Pian and Tong (1971). Atluri *et al*. (1975) proposed the first three-field hybrid element for fracture mechanic applications. In most of the elementary hybrid formulations, more than one element was needed to mesh around the crack tip (Schnack and Wolf 1978). This restriction removed by introduction of the so-called 'Super element' by Tong *et al*. (1973). Many investigations were undertaken to improve hybrid element formulation (Lin and Mar 1976, Pian and Moriya 1978).

In addition to the mentioned elements, there are a group of force-based finite elements, which computes the effects of crack on the structural stiffness, based on the fracture mechanic laws, instead of modeling the crack itself. It is obvious that cracking reduces the structure stiffness locally. It is equivalent to increase in the local flexibility from the force formulation standpoint. The additional flexibility can be computed from the strain energy that is released due to cracking, based on the fracture mechanic laws. This technique, which is called local flexibility approach, is presented by Okamura *et al*. (1973). However, these type of elements cannot model cracks as an independent phenomenon, but they have their own capabilities. For example, analyzing cracked structures using these elements provide enough accurate responses. Because the crack is modeled by only one force-based element, using these elements reduces degrees of freedom in comparison to the other elements such as QPEs. Moreover, this method is useful for vibration-based crack detection, in which the same structure is analyzed many times assuming various locations and depths for cracks. In this situation, using the finite elements derived based on the local flexibility approach removes the inevitability to remesh the structure. Since the introduction of this method by Okamura *et al*. (1973), various researchers proposed different cracked beam and plane elements using this approach (Saavedra and Cuitino 2001, Kisa 2012, Ibrahim *et al*. 2013, Akbas 2015, Viola *et al*. 2002, Bouboulas and Anifantis 2008, Skrinar, 2013, Krawczuk 1993, Rezaiee-Pajand and Gharaei-Moghaddam 2017, Rezaiee-Pajand and Mousavi 2009, Salah *et al*. 2014, Liu and Shu 2015, Yalaci 2016).

The first element of this type for plane problems is proposed by Krawczuk (1993). He formulated a 4-node quadrilateral plane finite element containing an edge crack. This element demonstrates acceptable accuracy in analysis of the cracked plane problems. The main shortcoming of this element is that the crack must be necessarily located vertically in the middle of the element. In addition, rectangular geometry provides difficulties in meshing different geometries. In another research work, Rezaiee-Pajand and Mousavi (2009) suggested a three-node triangular cracked element. Their element possesses linear displacement and constant strain fields. Like Krawczuk *et al*. formulation (1993), the independent forces are taken along the three sides of the element. Similar to the previous element, in this formulation, crack must be located in the center of the element, and it also needs to be vertical. Therefore, for inclined cracks, the element itself must be rotated. This restriction, which causes difficulties in meshing the structures with inclined cracks, can be easily removed by choosing an appropriate basic coordinate system. In addition to this drawback, the assumption of the constant stress field results in poor responses, especially, when the crack depth size is noticeable in comparison to the element dimensions. Rezaiee-Pajand and Mousavi used this element for the damage detection in gravitational dams. In the most recent research work in this field, Rezaiee-Pajand and Gharaei-Moghaddam (2017) proposed a general quadrilateral cracked element, which can model arbitrarily inclined cracks. They also proposed a new method to compute stress intensity factors of the cracked structures. Despite this major improvement, the quadrilateral geometry of this element causes difficulties in meshing structures, yet.

In addition to the plane elements, this type of formulation is also utilized for development of cracked beam elements. In application of the compliance concept to formulation of the cracked elements, Kisa *et al*. (1998) integrates the local flexibility approach and component mode synthesis to analyze free vibration behavior of cracked Timoshenko beams. Their method is proved to be an efficient and effective approach in comparison to the previous finite element studies. In another study, Kisa and Brandon (2000) studied effects of the crack closure on dynamic responses of a cracked beam. They computed stiffness matrix of the cracked element by addition of the stiffness matrix of a rotational spring, which was used to model the crack, to the non-cracked beam stiffness. In order to include the effects of the closure in the formulation, they utilized a novel approach. These investigators modeled the contact at the crack surface by two independent linear springs in the normal and tangential direction and compute another additional stiffness according to the actions of these springs.

One of the researchers who performed many constructive studies in this field is Akbas. In one of his research works, post buckling behavior of the cracked cantilever beam made of functionally graded materials is investigated (Akbas 2015b). In this study, the crack is modeled by a massless rotational spring, which connects the non-cracked parts of the beam together. In this work, the geometrical nonlinearities are included by taking advantage of total Lagrangian formulation. The objective of this paper was to evaluate effects of the crack location and depth on the post-buckling behavior of the beam. Later, Akbas developed the previous research, by investigating the situation in which the cracked cantilever beam is subjected to a non-follower axial load (Akbas 2016a). In this research, the differences between post-buckling behavior of the cracked and non-cracked beams are further investigated. Due to utilization of the von-Karman strain-displacement relations in the formulation, there is no limitation on the magnitude of the displacements and rotations. Akbas utilized similar formulation in order to study the response of an edge cracked cantilever beam to an impact force (Akbas 2014). Once again, the effects of the crack are included by the local flexibility approach. In this study, the vibration problem is solved in the time domain and effects of the

crack depth and location on the properties of the reflected wave is investigated. In a different study, Akbas investigated static bending of edge cracked micro beams by modification of the classic cracked beam theory based on replacing the crack with a rotational spring (Akbas 2016b)

In another work about the effects of the transverse crack on the dynamic responses of laminated composite beams, Behara *et al*. (2015) formulated a cracked Timoshenko beam element based on the first-order shear deformation theory and the compliance concept. In this study, the effects of various parameters, such as, fiber orientation, crack depth and crack location on natural frequencies of the cracked beam are investigated.

In one of the most-recent studies in this field, Zeng *et al*. (2017) simulate dynamic behavior of the cracked cantilever beams by using ANSYS. In this research work, they considered both stable and propagating cracks and models the cracked structures using the combination of the beam and solid elements. An advantage of this study is inclusion of the crack breathing behavior by definition of the contact pressure distribution over the crack surface.

This type of formulation is also utilized for analysis of damaged composite beams Fan and Wang (2015) evaluated vibrations of a laminated beam made of composite layers reinforced with carbon nanotubes and containing cracks in its matrix. The beam was formulated by using the Euler-Bernoulli beam theory, and the perturbation approach was used to solve its equation of motion. They found out that the extent of the crack plays a role in the linear vibration, but its influence on the nonlinear vibrations is less noticeable.

Since the early research works in this field until now, considerable developments have been achieved. However, there are still more problems to be solved. One of these difficulties, is to find an accurate and practical method for crack detection. By using *X*-ray and ultra-sound waves for the damage detection, very acceptable results are achieved, but these approaches, which are called direct methods, are too expensive, and therefore, their applications are not very feasible. An alternative way for the crack detection is the inverse method by using FEM analysis. The inverse scheme is based on this fact that the presence of crack alters free vibration responses of structures. In this method, by performing consecutive free vibration analyses for various crack locations and depths, the exact location and depth of the crack or cracks are specified. According to this definition, it is obvious that appropriate finite elements for this method must have the important properties of accuracy and efficiency. The special crack tip elements, such, as quarter-point and hybrid elements provide very accurate responses, but the necessity to remesh structure consecutively, diminishes efficiency of these elements. Therefore, the only available candidates are the cracked elements formulated based on the local flexibility approach. Because in this formulation, the cracks are located in the element and are not modeled as a unique phenomenon, there is no need to remesh structure in the successive analysis. Based on this fact, the goal of this study is to propose two new cracked plane elements. Although, the element previously proposed by Rezaiee-Pajand and Mousavi (2009) has triangular geometry, but the assumption of the constant stress-field within the element descends it accuracy considerably. To remove this problem, in this paper, two triangular cracked elements are proposed. These elements, with three and six nodes, possess constant and linear strain fields, respectively. It is obvious that because of the rigid body motions, there is no flexibility matrix for the elements in the global coordinates. Consequently, like other force-based elements, a basic coordinate system is opted. The basic system is originated in the center of the crack and one of its axes is in the crack direction. This setup removes the necessity of central vertical crack of the previously mentioned force-based element (Rezaiee-Pajand and Mousavi 2013). It is well-known that triangular geometry of the elements provides benefits in meshing structures. The suggested finite elements are applicable for static, dynamic and free vibration analysis of structures. In addition, the proposed elements are applicable for direct stress intensity calculation, which is a great advantage in comparison with the other similar elements. Moreover, the simple formulation of the three-node element makes it appropriate for educational purposes, as well. Various numerical examples demonstrate accuracy of the formulation. It must be noted that the ability of the suggested elements in capturing natural frequencies of cracked structures with acceptable accuracy makes them appropriate for vibration-based crack detection techniques.

The paper is organized in the following form: formulations of the non-cracked elements are included in section 2. The computations of the additional flexibility matrix caused by cracks are presented in section 3. Section 4, presents the necessary steps to compute the element mass matrix in the global coordinates. In section 5, a brief review of the element proposed by Rezaiee-Pajand and Mousavi is presented. Section 6 contains numerical evaluation of the presented elements, and the conclusion is made in section 7.

2. Formulation of the non-cracked elements

In this section, formulation of the non-cracked elements on the basic coordinate system or presented.

2.1 Three-node triangular element

In this subsection, a three-node triangular element with internal open crack will be formulated. As discussed earlier,

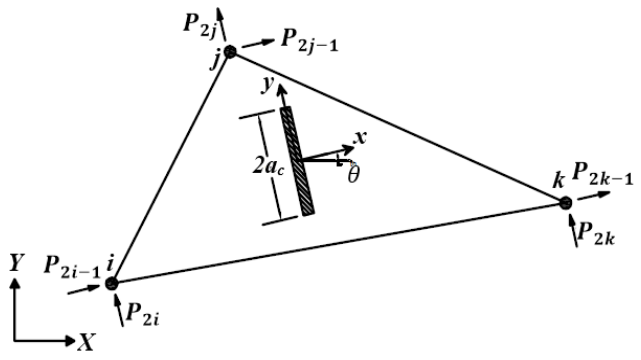

Fig. 1 Three-node triangular element in the global and basic coordinates

there is no flexibility matrix for the element in the global coordinate because of dependent degrees of freedom. Therefore, a basic coordinate system is selected, and only independent nodal forces will be used. Fig. 1 demonstrates the element in the Global (*XY*) and local basic coordinates (*xy*). The formulation starts by selection of the dependent and independent degrees of freedom, which are addressed by P_r and P_b, respectively

$$\{P_r\} = \{P_{2i-1} \quad P_{2i} \quad P_{2k}\}^T \tag{1}$$

$$\{P_b\} = \{P_{2j-1} \quad P_{2j} \quad P_{2k-1}\}^T = \{P_{b_1} \quad P_{b_2} \quad P_{b_3}\}^T \tag{2}$$

These two sets of forces are related to each other by the following equation

$$\{P_r\} = [T]\{P_b\} \tag{3}$$

$$[T] = \begin{bmatrix} -1 & 0 & -1 \\ \frac{y_{ij}}{x_{ki}} & \frac{x_{ji}}{x_{ki}} - 1 & \frac{y_{ik}}{x_{ki}} \\ \frac{y_{ji}}{x_{ki}} & \frac{x_{ij}}{x_{ki}} & \frac{y_{ki}}{x_{ki}} \end{bmatrix} \tag{4}$$

The subscript $\alpha\beta$ for coordinates will henceforth be used to represent the difference between two same quantities related to nodes α and β, as follows

$$(.)_{\alpha\beta} = (.)_\alpha - (.)_\beta \qquad \alpha, \beta = i, j, k \tag{5}$$

In the basic system, the following shape function interpolates the displacement fields of the element

$$N_\alpha = \frac{1}{2A_{el}}(a_\alpha + b_\alpha x + c_\alpha y) \qquad \alpha = i, j, k \tag{6}$$

The coefficients in Eq. (6) are defined as follows

$$A_{el} = \frac{1}{2}\left(x_i y_j + x_j y_k + x_k y_i - x_i y_k - x_j y_i - x_k y_j\right) \tag{7}$$

$$a_\alpha = \frac{1}{2} e_{\alpha\beta\gamma}\left(x_\beta y_\gamma - x_\gamma y_\beta\right) \qquad \alpha, \beta, \gamma = i, j, k \tag{8}$$

$$b_\alpha = \frac{1}{2} e_{\alpha\beta\gamma}(y_\beta - y_\gamma) \qquad \alpha, \beta, \gamma = i, j, k \tag{9}$$

$$c_\alpha = \frac{1}{2} e_{\alpha\beta\gamma}(x_\gamma - x_\beta) \qquad \alpha, \beta, \gamma = i, j, k \tag{10}$$

In the presented relations, $\boldsymbol{e_{\alpha\beta\gamma}}$ is the Levi-Civita tensor. To derive the flexibility matrix of the element, the relationship between strains and independent nodal displacements is needed. This relation is presented by following equation

$$\{\varepsilon\} = \begin{Bmatrix} \varepsilon_x \\ \varepsilon_y \\ \varepsilon_{xy} \end{Bmatrix} = \begin{bmatrix} \frac{\partial}{\partial x} & 0 \\ 0 & \frac{\partial}{\partial y} \\ \frac{\partial}{\partial y} & \frac{\partial}{\partial x} \end{bmatrix} \begin{bmatrix} N_j & 0 & N_k \\ 0 & N_j & 0 \end{bmatrix} \begin{Bmatrix} D_{2j-1} \\ D_{2j} \\ D_{2k-1} \end{Bmatrix} \tag{11}$$

$$= [B]\{D_b\}$$

$$[B] = \begin{bmatrix} b_j & 0 & b_k \\ 0 & c_j & 0 \\ c_j & b_j & c_k \end{bmatrix} \tag{12}$$

Now, the stiffness matrix of the non-cracked element is derived using the succeeding relation

$$[S_b] = \int_V [B]^T [D_m][B] dV \tag{13}$$

where D_m is the material matrix and is defined in the next form

$$[D_m] = \frac{E}{(1-\nu^2)} \begin{bmatrix} 1 & \nu & 0 \\ \nu & 1 & 0 \\ 0 & 0 & \frac{(1-\nu)}{2} \end{bmatrix} \tag{14}$$

Replacing Eqs. (12) and (14) in Eq. (13) and inverting the resulted stiffness matrix leads to the following flexibility matrix for the non-cracked element

$$\left[{F_b}^0\right] = [S_b]^{-1} = \begin{bmatrix} {f^0}_{11} & {f^0}_{12} & {f^0}_{13} \\ {f^0}_{21} & {f^0}_{22} & {f^0}_{23} \\ {f^0}_{31} & {f^0}_{32} & {f^0}_{33} \end{bmatrix} \tag{15}$$

In which

$$\begin{gathered} {f^0}_{11} = \frac{Q_3}{k.Q_1.{Q_2}^2} \\ {f^0}_{12} = f_{12} = \frac{Q_4}{k.Q_1.Q_2} \\ {f^0}_{13} = f_{31} = \frac{-Q_5}{k.Q_1.{Q_2}^2} \\ {f^0}_{22} = \frac{1}{k.Q_1} \\ {f^0}_{23} = f_{32} = \frac{Q_6}{k.Q_1.Q_2} \\ {f^0}_{33} = \frac{Q_7}{k.Q_1.{Q_2}^2} \end{gathered} \tag{16}$$

Where the intermediate parameters are defined as comes in the next lines

$$\begin{gathered} k = \frac{AEt}{4{A_{el}}^2} \\ Q_1 = c_j^2 \\ Q_2 = b_j.c_k - b_k.c_j \\ Q_3 = c_j^2(b_k^2 + c_k^2) + b_k^2(b_j^2 + c_j^2) \\ +2\nu(b_k^2.c_j^2 - b_j.c_j.b_k.c_k) \\ Q_4 = b_j.b_k - c_j.c_k.\nu \\ Q_5 = b_j^3.b_k + c_j^2(c_j.c_k + 2b_j.b_k) \\ +\nu(b_j.b_k.c_j^2 - c_j.c_k.b_j^2) \\ Q_6 = c_j^2.\nu - b_j^2 \\ Q_7 = (b_j^2 + c_j^2)^2 \end{gathered} \tag{17}$$

In these relation, t and A are thickness and area of the element.

2.2 Six-node triangular element

The same formulation steps are undertaken for the six-node element which is demonstrated in Fig. 2. It should be noted that there are only three sets of the independent nodal coordinates in the formulation of six-node element. Because the additional three nodes are placed in the mid-sides, and

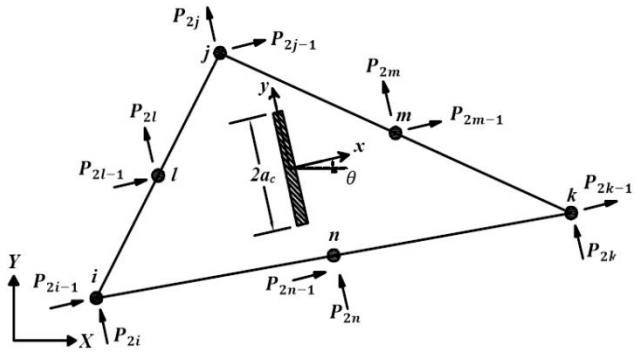

Fig. 2 Six-node triangular element in the global and basic coordinates

their coordinates are dependent to the vertex nodes.

Dependent and independent degrees of freedom and their connecting equation for the six-node element are as follows

$$\{P_r\} = \{P_{2i-1} \quad P_{2i} \quad P_{2k}\}^T \tag{18}$$

$$\{P_b\} = \{P_{2j-1}\ P_{2j}\ P_{2k-1}\ \ P_{2l-1}\ \ P_{2l}\ \ P_{2m-1}\ \ P_{2m}\ \ P_{2n-1}\ \ P_{2n}\}^T \tag{19}$$

$$\{P_r\} = [T]\{P_b\} \tag{20}$$

$$[T] = \begin{bmatrix} -1 & 0 & -1 & -1 & 0 \\ \frac{y_{ij}}{x_{ki}} & \frac{x_{ji}}{x_{ki}} - 1 & \frac{y_{ik}}{x_{ki}} & \frac{y_{ij}}{2x_{ki}} & \frac{x_{ji}}{2x_{ki}} - 1 \\ \frac{y_{ji}}{x_{ki}} & \frac{x_{ij}}{x_{ki}} & \frac{y_{ki}}{x_{ki}} & \frac{y_{ji}}{2x_{ki}} & \frac{x_{ij}}{2x_{ki}} \\ -1 & 0 & -1 & 0 & \\ \frac{(y_{ij}+y_{ik})}{2x_{ki}} & \frac{(x_{ji}+x_{ki})}{2x_{ki}} - 1 & \frac{y_{ik}}{2x_{ki}} & \frac{-1}{2} & \\ \frac{(y_{ji}+y_{ki})}{2x_{ki}} & \frac{(x_{ij}+x_{ik})}{2x_{ki}} & \frac{y_{ki}}{2x_{ki}} & \frac{-1}{2} & \end{bmatrix} \tag{21}$$

The following shape functions interpolate displacement fields of the six-node element

$$N_\alpha = n_{\alpha1} + n_{\alpha2}.x + n_{\alpha3}.y + n_{\alpha4}.xy + n_{\alpha5}.x^2 + n_{\alpha6}.y^2 \qquad \alpha = i,j,k,l,m,n \tag{22}$$

The coefficients of the mentioned equation are derived using the next relations

$$\begin{cases} n_{\alpha1} = \frac{1}{4A_{el}^2}(2a_\alpha^2 - a_\alpha A_{el}) \\ n_{\alpha2} = \frac{1}{4A_{el}^2}(4a_\alpha b_\alpha - b_\alpha A_{el}) \\ n_{\alpha3} = \frac{1}{4A_{el}^2}(4a_\alpha c_\alpha - c_\alpha A_{el}) \\ n_{\alpha4} = \frac{1}{4A_{el}^2}(4b_\alpha c_\alpha) \\ n_{\alpha5} = \frac{1}{4A_{el}^2}(2b_\alpha^2) \\ n_{\alpha6} = \frac{1}{4A_{el}^2}(2c_\alpha^2) \end{cases} \quad for\ \alpha = i,j,k \tag{23}$$

$$\begin{cases} n_{\alpha1} = \frac{1}{A_{el}^2}(a_\beta a_\gamma) \\ n_{\alpha2} = \frac{1}{A_{el}^2}(a_\beta b_\gamma + a_\gamma b_\beta) \\ n_{\alpha3} = \frac{1}{A_{el}^2}(a_\beta c_\gamma + a_\gamma c_\beta) \\ n_{\alpha4} = \frac{1}{A_{el}^2}(b_\beta c_\gamma + b_\gamma c_\beta) \\ n_{\alpha5} = \frac{1}{A_{el}^2}(b_\beta b_\gamma) \\ n_{\alpha6} = \frac{1}{A_{el}^2}(c_\beta c_\gamma) \end{cases} \quad for\ \alpha = l \tag{24}$$

$$\rightarrow \begin{cases} \beta = i \\ \gamma = j \end{cases}, \quad \alpha = m \rightarrow \begin{cases} \beta = j \\ \gamma = k \end{cases}, \quad \alpha = n \rightarrow \begin{cases} \beta = k \\ \gamma = i \end{cases}$$

The Following relations will be used to compute the non-cracked six-node element stiffness matrix in the basic coordinate system

$$\{\varepsilon\} = \begin{Bmatrix} \varepsilon_x \\ \varepsilon_y \\ \varepsilon_{xy} \end{Bmatrix} = \begin{bmatrix} \frac{\partial}{\partial x} & 0 \\ 0 & \frac{\partial}{\partial y} \\ \frac{\partial}{\partial y} & \frac{\partial}{\partial x} \end{bmatrix} \begin{bmatrix} N_j & 0 & N_k & N_l & 0 & N_m & 0 & N_n & 0 \\ 0 & N_j & 0 & 0 & N_l & 0 & N_m & 0 & N_n \end{bmatrix} \{D_b\} = [B]\{D_b\} \tag{25}$$

$$[S_b] = \int_V [B]^T[D_m][B]dV = t.\int_A [B]^T[D_m][B]dA = t.\int_A [IN]dA \tag{26}$$

The elements of the integrand in the previous equation, are all second-order polynomial functions of coordinates x and y. Using Gauss integration scheme, with three quadrature points, provides exact results for the integral of Eq. (26). Finally, the non-cracked flexibility matrix of the element is computed by inverting its stiffness

$$[F_b{}^0] = [S_b]^{-1} \tag{27}$$

3. Derivation of the additional flexibility matrix

The additional flexibility matrix due to crack is derived from the following equation, according to the principles of linear elastic fracture mechanics (LEFM)

$$[\boldsymbol{F_b^1}] = \frac{\partial^2 U^r}{\partial P_{b_i} \partial P_{b_j}} \tag{28}$$

In this equation, U^r is the released strain energy due to crack, which can be derived in terms of stress intensity factors

$$U^r = \frac{1}{E}\int_{A_c} ({K_I}_A{}^2 + {K_I}_B{}^2 + {K_{II}}_A{}^2 + {K_{II}}_B{}^2) \tag{29}$$

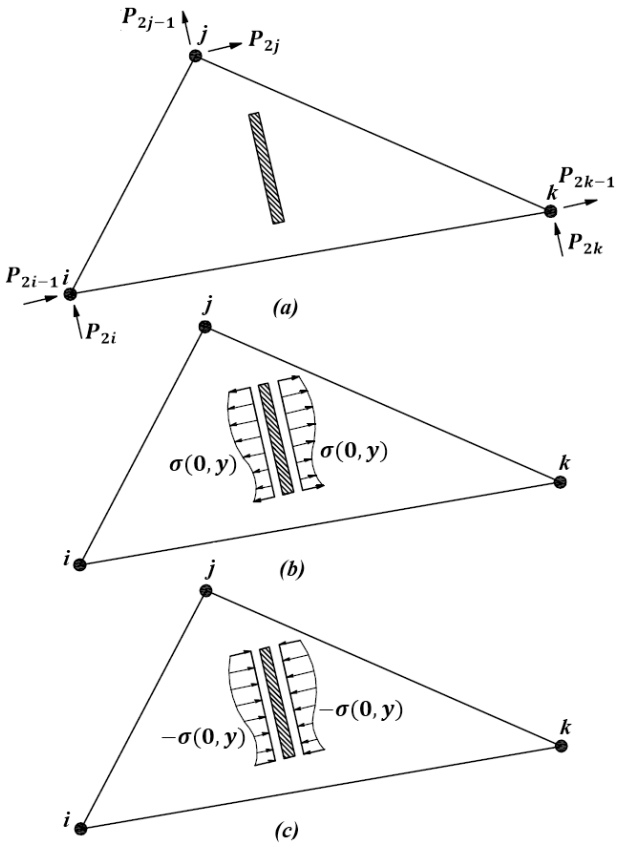

Fig. 3 Various loading states of the cracked element

where, A and B stands for the two crack tips. K_I and K_{II} are the stress intensity factors of the opening and the sliding fracture modes, respectively and Ac is the crack surface area.

To compute the stress intensity factor of the element, three loading states, demonstrated in Fig. 3, are considered.

Fig. 3(a) is the element under nodal forces. The nodal forces lead to the stress distributions on the crack surfaces, which are shown in Fig. 3(b). Fig. 3(c) is the same stress distribution but in the opposite direction. Based on the linear fracture mechanics' rule and superposition method, stress intensity factor of the cracked element is derived using the following relations

$$K = K_a + K_b + K_c \tag{30}$$

$$K_a + K_c = 0 \;\rightarrow\; K = K_c \tag{31}$$

Now, appropriate relations for stress intensity factors should be elected. In this study, the weight function approach is used. If the weight functions for a crack are in hand, the stress intensity factor can be derived from the following relation

$$\begin{Bmatrix} K_I \\ K_{II} \end{Bmatrix} = \int_{-a}^{a} \begin{bmatrix} h_{11}(y,a) & h_{12}(y,a) \\ h_{21}(y,a) & h_{22}(y,a) \end{bmatrix} \begin{Bmatrix} \sigma_x(0,y) \\ \tau_{xy}(0,y) \end{Bmatrix} dy \tag{32}$$

where, h_{ij} are the weight functions. The next equation can be used for calculation of the weight functions

$$h_{ij}(y,a) = \sqrt{\frac{1}{\pi a}} \sum_{n=0}^{\infty} D_n^{(ij)} \left(\frac{1}{2} + \frac{y}{2a}\right)^{n-\frac{1}{2}} \tag{33}$$

To achieve an acceptable accuracy, first few expressions of this power series suffice. In this study, the first three term of the series is used; therefore, the previous relation can be rewritten in the next form

$$h_{ij}(y,a) \cong \sqrt{\frac{1}{\pi a}} \left[D_0^{(ij)} \left(\frac{1}{2} + \frac{y}{2a}\right)^{-\frac{1}{2}} + D_1^{(ij)} \left(\frac{1}{2} + \frac{y}{2a}\right)^{\frac{1}{2}} + D_2^{(ij)} \left(\frac{1}{2} + \frac{y}{2a}\right)^{\frac{3}{2}} \right] \tag{34}$$

In this equation, the coefficients $D_n^{(ij)}$ are functions of the angle between the crack direction and the coordinate axis. For the case that this angle is zero, like this study, $D_n^{(12)}$ and $D_n^{(21)}$ are equal to zero, and the Eq. (35) becomes uncoupled

$$\begin{Bmatrix} K_I \\ K_{II} \end{Bmatrix} = \int_{-a}^{a} \begin{bmatrix} h_{11}(y,a) & 0 \\ 0 & h_{22}(y,a) \end{bmatrix} \begin{Bmatrix} \sigma_x(0,y) \\ \tau_{xy}(0,y) \end{Bmatrix} dy \tag{35}$$

The coefficients for the other two weight functions are computed by various researchers for edge and internal cracks at different angles. In this study, the following coefficients are used in for edge cracks (Fett and Munz 1997)

$$\begin{cases} D_0^{(11)} = D_0^{(22)} = 1 \\ D_1^{(11)} = D_1^{(22)} = 0.568 \\ D_2^{(11)} = D_2^{(22)} = 0.283 \end{cases} \tag{36}$$

According to Eq. (28), the additional flexibility for the three-node element is computed using the succeeding equation

$$\left[F_b{}^1\right] = \frac{\partial^2 U}{\partial P_{b_i} \partial P_{b_j}} = \begin{bmatrix} f^1{}_{11} & f^1{}_{12} & f^1{}_{13} \\ f^1{}_{21} & f^1{}_{22} & f^1{}_{23} \\ f^1{}_{31} & f^1{}_{32} & f^1{}_{33} \end{bmatrix} \tag{37}$$

For the six-node element this would be a 9×9 matrix.

It is needed to take derivatives of the released strain energy with respect to the basic forces to compute additional flexibility based on Eq. (37). Therefore, the stresses are calculated as a function of the basic nodal forces. For this purpose, the following relations are established

$$\{\sigma\} = \begin{Bmatrix} \sigma_x \\ \sigma_y \\ \tau_{xy} \end{Bmatrix} = [D_m]\{\varepsilon\} = \frac{E}{(1-\nu^2)} \begin{bmatrix} 1 & \nu & 0 \\ \nu & 1 & 0 \\ 0 & 0 & \frac{(1-\nu)}{2} \end{bmatrix} \begin{Bmatrix} \varepsilon_x \\ \varepsilon_y \\ \varepsilon_{xy} \end{Bmatrix} \tag{38}$$

$$\{D_b\} = \left[F_b{}^0\right]\{P_b\} \tag{39}$$

$$\{\sigma\} = [D_m]\{\varepsilon\} = [D_m][B]\{D_b\} = [D_m][B][F_b]\{P_b\} = [\mathrm{I}]\{P_b\} \tag{40}$$

For the three-node element, the stress interpolation matrix can be derived as follows

$$[\mathbf{I}] = \begin{bmatrix} I_{11} & I_{12} & I_{13} \\ I_{21} & I_{22} & I_{23} \\ I_{31} & I_{32} & I_{33} \end{bmatrix} = \frac{\mathrm{A}_{el}}{A.t.Q_1.Q_2{}^2.(\nu^2-1)} *$$

$$\begin{bmatrix} -2(b_j.Q_3 - b_k.Q_5 + c_j.Q_2.Q_4.\nu) \\ -2((b_j.Q_3 - b_k.Q_5).\nu + c_j.Q_2.Q_4) \\ (c_j.Q_3 - c_k.Q_5 + b_j.Q_2.Q_4).(\nu - 1) \end{bmatrix}$$
$$-2Q_2(b_j.Q_4 + b_k.Q_6 + c_j.Q_2.\nu)$$
$$-2Q_2((b_j.Q_4 + b_k.Q_6).\nu + c_j.Q_2) \quad (41)$$
$$Q_2(c_j.Q_4 + c_k.Q_6 + b_j.Q_2).(\nu - 1)$$
$$\begin{bmatrix} -2(b_k.Q_7 - b_j.Q_5 + c_j.Q_2.Q_6.\nu) \\ -2((b_k.Q_7 - b_j.Q_5).\nu + c_j.Q_2.Q_6) \\ (c_k.Q_7 - c_j.Q_5 + b_j.Q_2.Q_6).(\nu - 1) \end{bmatrix}$$

Therefore, the Eq. (35) can be expanded in the following form

$$\begin{Bmatrix} K_I \\ K_{II} \end{Bmatrix} = \sqrt{\frac{1}{\pi a}} \int_{-a}^{a} \left[\left(\frac{1}{2} + \frac{y}{2a}\right)^{-\frac{1}{2}} + 0.568 \left(\frac{1}{2} + \frac{y}{2a}\right)^{\frac{1}{2}} \right.$$
$$\left. + 0.283 \left(\frac{1}{2} + \frac{y}{2a}\right)^{\frac{3}{2}} \right] \begin{bmatrix} I1(0,y) \\ I3(0,y) \end{bmatrix} . \{P_b\} dyy \quad (42)$$

where $I1$ and $I3$ are the first and the third rows of $[I(\mathbf{0}, \boldsymbol{y})]$. Now by replacing this relation in Eq. (37) and taking derivatives with respect to the basic forces, the additional flexibility matrix will be computed. Consequently, the flexibility matrix of the element in basic coordinates is computed by the following equation

$$[F_b] = [F_b{}^0] + [F_b{}^1] \quad (43)$$

In the coming sections, a method for calculating the element stiffness matrix in global coordinates will be presented.

4. Computation of global stiffness matrix

Due to shortcomings of the pure force-based methods in the structural analysis, it is preferred to compute the stiffness of the element by inverting the flexibility matrix and solve problems in the conventional displacement-based framework. In the local or basic coordinates, the following relation connects the dependent and independent degrees of freedom to each other

$$\begin{Bmatrix} P_b \\ P_r \end{Bmatrix} = \begin{bmatrix} S_{bb} & S_{br} \\ S_{rb} & S_{rr} \end{bmatrix} \begin{Bmatrix} D_b \\ D_r \end{Bmatrix} \quad (44)$$

It is helpful to remind that b and r subscripts indicate parameters, which belong to the basic or independent degrees of freedom and rigid body or independent ones, respectively. The next relations are held in the basic coordinates

$$\{\mathrm{P_b}\} = [\mathrm{F_b}]^{-1}\{\mathrm{D_b}\} \quad (45)$$

$$[S_{bb}] = [F_b]^{-1} \quad (46)$$

Eq. (3) can be rewritten in the following form by taking advantage of Eq. (46)

$$\{P_r\} = [T][S_{bb}]\{D_d\} = [T][F_b]^{-1}\{D_b\} \quad (47)$$

$$[S_{rb}] = [T][F_b]^{-1} \quad (48)$$

From the symmetry property of stiffness matrix, following equation is deduced

$$[S_{br}] = [S_{rb}]^T = [F_b]^{-1}[T]^T \quad (49)$$

And S_{rr} is derived as follows

$$\{P_r\} = [T]\{P_b\} = [T][S_{br}]\{D_r\} \quad (50)$$

$$[S_{rr}] = [T][F_b]^{-T}[T]^T \quad (51)$$

Therefore, the local stiffness matrix is derived in the coming form

$$[S]_{EL} = \begin{bmatrix} [F_b]^{-1} & [F_b]^{-1}[T]^T \\ [T][F_b]^{-1} & [T][F_b]^{-1}[T]^T \end{bmatrix} \quad (52)$$

Finally, the global stiffness matrix of the element is obtained by taking advantage of transformation matrix R

$$[S]_{EG} = [R]^T[S]_{EL}[R] \quad (53)$$

$$[R] = \begin{bmatrix} R_j & 0 & 0 \\ 0 & R_j & 0 \\ 0 & 0 & R_j \end{bmatrix} \quad (54)$$

$$[R_j] = \begin{bmatrix} cos(\theta) & sin(\theta) \\ -sin(\theta) & cos(\theta) \end{bmatrix} \quad (55)$$

5. Rezaiee-Pajand and Mousavi element

As mentioned earlier, the first triangular cracked element using force method is proposed by Rezaiee-Pajand and Mousavi (2009). While this research work is published in Persian, it would be helpful to bring a brief summary of this formulation in this section. Fig. 4 shows the element. It is evident that the crack must be placed exactly in the center of the element, and also it must be vertical.

Side forces are selected as independent forces and it is assumed that the stresses in the element are constant. Based on the force formulation method, non-cracked flexibility for the independent degrees of freedom is derived as presented in Eq. (56)

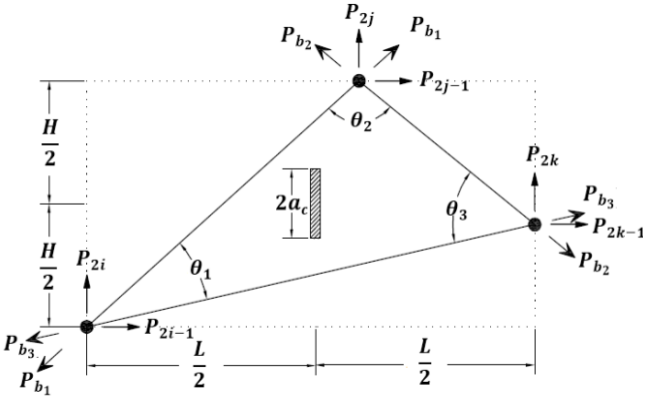

Fig. 4 Cracked triangular element proposed by Rezaiee-Pajand and Mousavi

$$[F_b{}^0] = \frac{2}{Et}\begin{bmatrix} \frac{sin\theta_3}{sin\theta_1 sin\theta_2} & cos\theta_2 cot\theta_2 - \nu.sin\theta_2 & cos\theta_1 cot\theta_1 - \nu.sin\theta_1 \\ cos\theta_2 cot\theta_2 - \nu.sin\theta_2 & \frac{sin\theta_1}{sin\theta_3 sin\theta_2} & cos\theta_3 cot\theta_3 - \nu.sin\theta_3 \\ cos\theta_1 cot\theta_1 - \nu.sin\theta_1 & cos\theta_3 cot\theta_3 - \nu.sin\theta_3 & \frac{sin\theta_2}{sin\theta_1 sin\theta_3} \end{bmatrix} \quad (56)$$

To compute the additional flexibility matrix, the authors took advantage of the Eq. (28), while they used different stress intensity factor. To consider the effect of the inelastic area at the crack tip, they used Irwin's model and computed inelastic stress intensity factors as follows

$$K_I = K_{Ie}\sqrt{1 + \frac{g^2\left(\frac{a}{W}\right)}{\pi}\left(\frac{\sigma_x}{\sigma_{yi}}\right)^2} \quad (57)$$

$$K_{II} = K_{IIe}\sqrt{1 + \frac{g^2\left(\frac{a}{W}\right)}{\pi}\left(\frac{\tau_{xy}}{\sigma_{yi}}\right)^2} \quad (58)$$

Where $\boldsymbol{\sigma_{yi}}$ is the material yield stress and $\boldsymbol{K_{Ie}}$ and $\boldsymbol{K_{IIe}}$ are elastic stress intensity factors which are defined in the following form

$$K_{Ie} = \frac{1}{\sqrt{\pi a}}\int_{-a}^{a}\sigma_x(0,y)\sqrt{\frac{a+y}{a-y}}dy \quad (59)$$

$$K_{IIe} = \frac{-1}{\sqrt{\pi a}}\int_{-a}^{a}\tau_{xy}(0,y)\sqrt{\frac{a+y}{a-y}}dy \quad (60)$$

Based on the constant stress assumption, the stresses needed in Eqs. (59) and (60), are derived from the next relations

$$\sigma_X = \frac{2}{t}\left[\frac{{l_{12}}^2}{h_3}P_{b_1} + \frac{{l_{23}}^2}{h_1}P_{b_2} + \frac{{l_{31}}^2}{h_2}P_{b_3}\right] \quad (61)$$

$$\tau_{XY} = \frac{2}{t}\left[\frac{l_{12}m_{12}}{h_3}P_{b_1} + \frac{l_{23}m_{23}}{h_1}P_{b_2} + \frac{l_{31}m_{31}}{h_2}P_{b_3}\right] \quad (62)$$

where $l_{\alpha\beta}$ and $m_{\alpha\beta}$ are the direction cosines of the triangle sides, and h_α is the height of the triangle with respect to the point α. Using these relations and Eq. (28) they computed the additional flexibility matrix in basic coordinates.

6. Numerical evaluations

To evaluate accuracy and capabilities of the proposed cracked elements, various numerical examples will be solved in this section. First, a problem without crack will be analyzed to verify the computed non-cracked flexibility matrices. Then, by computation of displacements, natural frequencies and stress intensity factor of some cracked structures, precision of the suggested elements will be studied and their accuracy will be compared with the other existing elements.

Table 1 Tip deflection of the non-cracked cantilever beam

Element Type	Tip Deflection	Error (%)	Number of elements	Analysis time (second)	Efficiency index
TC-CST element	-96.8828	3.1172	2048	1.7472	0.1835
TC-LST element	-99.8942	0.106	64	0.1266	74.52
R-M element	-96.4532	3.5468	2048	1.8752	0.1503

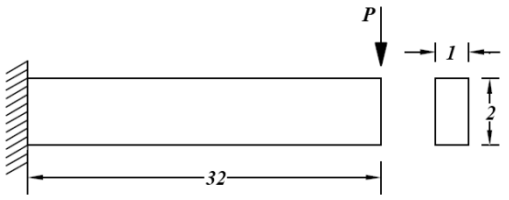

Fig. 5 Non-cracked cantilever beam under tip loading

6.1 A cantilever beam under tip loading

In the first numerical example, a cantilever beam under concentrated load at its free end will be analyzed. Fig. 5 demonstrates this beam.

The exact deflection of the beam tip under tip loading can be computed using the following relation

$$\Delta = \frac{PL^3}{3EI} + \frac{PL}{F_s.GA} \quad (63)$$

Where, E and G are the elastic and shear modulus of the beam materials. L and A are the beam length and cross section area, respectively, and Fs stands for the shear correction factor.

For the sake of simplicity, the problem quantities are dimensionless. Length of the beam is taken equal to 32 units and it has a 2×1 rectangular cross section. The shear correction factor for the rectangular sections is taken equal to $\frac{5}{6}$. The structure material has the modulus of elasticity equal to 7680 and its Poisson's ratio is 0.25. The tip load, P, is set to 46.7381. Therefore, using Eq. (63), the exact value for the tip deflection is equal to -100 units. The beam is analyzed using both suggested elements and also the triangular element proposed by Rezaiee-Pajand and Mousavi. The obtained results are presented in Table 1.

In Table 1, TC-CST and TC-LST stand for the triangular three-node and six-node elements, respectively, and R-M element is the element proposed by Rezaiee-Pajand and Mousavi (2009). The Efficiency index in the Table 1 is defined next

$$\text{Efficiency} = \frac{1}{Error} \times \frac{1}{Analysis\ time} \quad (64)$$

This index varies in the interval of (0, ∞). Greater index indicates that the element is more efficient. The attained responses verify accuracy of the non-cracked flexibility for both suggested elements. It is not a big surprise to observe that the six-node element is more accurate and efficient. It is also deduced from the obtained results, that Rezaiee-Pajand and Mousavi element is a bit less capable than the suggested new three-node triangular. Its lower efficiency is due to selection of the independent lateral forces in the present element that necessitate an additional

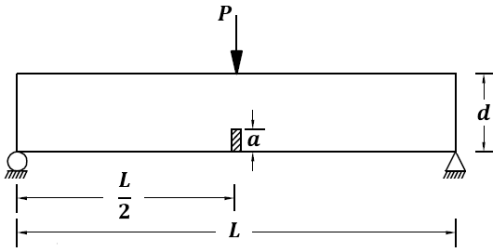

Fig. 6 Three-point bending specimen

Table 2 K_I/K_I^{Ref} of the three-point bending beam

a/d	Standard QP element (Guinea *et al*. 1998)	Improved QP element (Guinea *et al*. 1998)	TC-CST element	TC-LST element
0.1	1.0020	0.9981	0.9546	1.0045
0.2	0.9959	0.9995	0.9379	0.9964
0.3	0.9941	1.0011	0.8503	0.9841
0.4	0.9914	1.0011	0.8494	0.9532
0.5	0.9868	0.9990	0.7925	0.9312
0.6	0.9791	0.9946	0.7316	0.9206

transformation process to compute the local stiffness matrix.

6.2 Three-point bending specimen

In the third example, opening stress intensity factor for a three-point bending specimen is computed by the proposed elements. After finding the nodal displacements, the desired stress intensity factors are easily computed by taking advantage of Eq. (42). Fig. 6 demonstrates the specimen:

Length of the beam is selected 200 cm, and its height set to 25 cm. Its material modulus of elasticity and poison's ratio are equal to 210 GPa and 0.3, respectively. The applied load is equal to 0.2 kN. Guinea *et al*. (1998) proposed an approximating expression for stress intensity factor of a general three-point bending specimen that can be used as reference value in this example. In addition, Gray *et al*. (2003) analyzed a similar problem to evaluate their improved quarter point element. This structure is solved by using the suggested elements for a wide range of the crack length. All the results of the relative first mode stress intensity factor are listed in Table 2.

Deviation of the responses from the Reference value (Guinea *et al*. 1998) are depicted in Fig. 7. It is evident that the suggested elements are not accurate as the QP elements, because in the proposed formulation, only the effect of crack on structure flexibility is considered, and the crack is not treated as a unique physical phenomenon. Besides, it can be seen that the accuracy of the responses for almost all the studied elements decrease as the crack length increase, but the decrease in the suggested elements and especially the three-node one is faster. By considering all the mentioned results, it can be concluded that while deviation of the six-node element responses from the reference stress intensity factor for all a/d ratios lower than 0.4 is less than five percent, the element can be used for stress intensity computation of the short cracks with an acceptable accuracy.

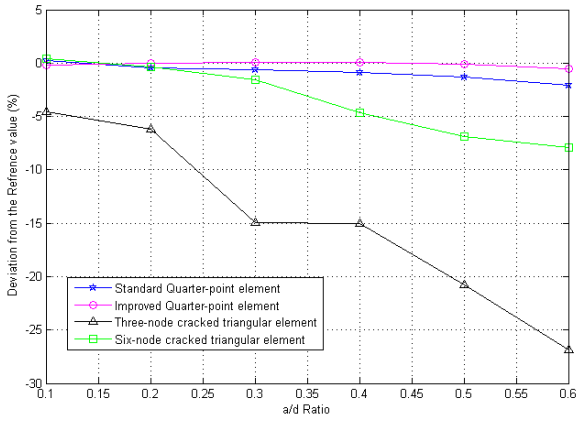

Fig. 7 Deviation of K_I from the Reference value

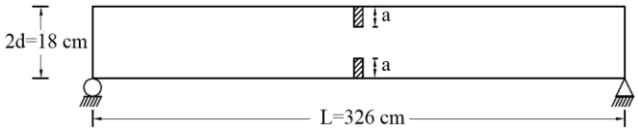

Fig. 8 Simple symmetrically cracked beam

Table 3 Natural frequencies of the symmetrically cracked beam

	a/d	Analytical (Charistidis and Bar 1984)	Fourier representation (Shen *et al*. 1990)	Krawczuk element (1993)	TC-CST element	TC-LST element
First Mode	1/2	0.8692	0.9134	0.8722	0.9532	0.8745
	1/3	0.9368	0.9679	0.9454	1.0025	0.9423
	1/4	0.9580	0.9811	0.9660	1.0048	0.9668
Second Mode	1/2	-	0.9996	1.0000	1.0252	0.9986
	1/3	-	0.9999	1.0021	1.0298	1.0017
	1/4	-	0.9999	1.0011	1.0332	1.0008
Third Mode	1/2	-	0.9251	0.8746	1.0023	0.8933
	1/3	-	0.9697	0.9471	1.0087	0.9319
	1/4	-	0.9818	0.9722	1.0126	0.9786

6.3 Natural vibration of a simple symmetrically cracked beam

To evaluate the ability of the suggested elements in the frequency computation, natural vibration of a simple beam with two cracks, which is shown in Fig. 8 is analyzed.

This beam is made of steel which its modulus of elasticity and poison's ratio are equal to 210 GPa and 0.3, respectively, and mass density is 7860 kg/m3. Previously, this problem was solved by Krawczuk (1993) and Shen *et al*. (1990). Also, Christidis and Bar (1984) computed first natural frequency of the beam analytically. The problem is analyzed using 2020 three-node elements and 62 six-node elements. The achieved responses of the three first modes of vibration for various ratios of a/d are presented in Table. 3. In addition, results of the previous references are offered.

The obtained results show acceptable accuracy of the proposed elements. As it was expected, the three-node element responses are not very accurate, because of constant stress assumption, which is a weak hypothesis. It must be stated that by using finer meshes, the accuracy of

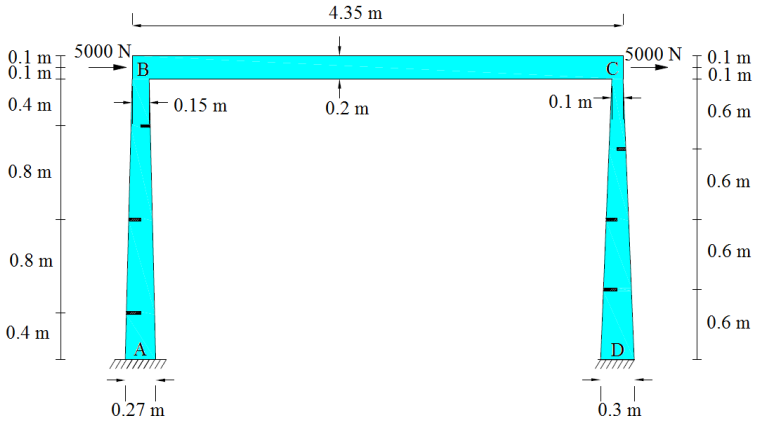

Fig. 9 Non-prismatic cracked frame

Table 4 Displacements and reactions of the non-prismatic frame

Parameter	Solution Method		
	Proposed element	Skrinar element (2013)	finite element program
Horizontal Displacement at B	6.8934 mm	6.9080 mm	6.9431 mm
Horizontal Displacement at C	6.8909 mm	6.9070 mm	6.9435 mm
Horizontal reaction at A	5118.2047 N	5117.4790 N	5115.7850 N
Moment reaction at A	8624.3650 N.m	8625.4860 N.m	8615.0248 N.m
Horizontal reaction at D	4881.7953 N	4882.5210 N	4884.2150 N
Moment reaction at D	8851.0260 N.m	8850.0310 N.m	8854.1200 N.m

the responses will not improve, because each crack is only modeled by one element. Another reason for the negligible existing error in the responses of the suggested elements is due to the stress intensity factor used for the formulation which belongs to a center crack instead of the edge cracks in this example.

6.4 A non-prismatic frame

To investigate the ability of the proposed element in analysis of cracked frames, the non-prismatic structure shown in Fig. 9 is analyzed.

Skrinar (2013) analyzed this structure to evaluate his cracked frame element. There are six edge cracks at the shown positions in the columns. Relative depth of all cracks is equal to 0.5. The material is assumed to be linear elastic with modulus of elasticity and Poisson's ratio equal to 30 GPa and 0.3, respectively. All structural members have rectangular cross section with 0.1 m thickness. The frame is loaded by two 5000 N horizontal nodal forces at points B and C at the beam ends.

This structure is modeled by using the six-node proposed element, and its nodal displacements and reactions are computed. The obtained results are presented in Table 4. In addition to the six-node suggested element, results of the Skrinar element and the responses attained by a general finite element program, which take advantage of embedded crack approach, are also inserted in Table 4.

It is evident that there is a good agreement between responses of the three different types of elements. Thus, accuracies of the new element in the static analysis of the cracked structures are suitable. It should be mentioned that 3215 six-node proposed elements are used to model this frame structure. To find these solutions, more than eight thousand Q8 elements are employed to mesh this problem with the finite element program. Q4 quarter-point elements are utilized for the crack tips.

7. Conclusions

Two triangular cracked elements, with thorough non-propagating cracks, are proposed. Both elements are formulated using the force method and the LEFM principles. One element is derived by assumption of the constant stress, and the other is formulated by assuming linear stress distribution. The main advantage of these elements is that they model the crack by only one element. This leads to a considerable decrease in the total degrees of freedom and computation time.

Various numerical examples evaluate the capability of the proposed elements in computation of the different responses, such as displacement, natural frequency and stress intensity factors. The obtained results lead to the following conclusions:

The suggested elements offer good accuracy for computation of the natural frequency belongs to the first modes of vibration; therefore, it can be utilized for vibration-based crack detection approaches. It is possible to take advantage of these types of cracked element for the stress intensity factor calculation.

The proposed elements are applicable to model structures with the same geometry but various crack lengths, without the need to re-mesh structure. This advantage provides a considerable time and computation effort saving and makes the elements applicable for inverse crack detection methods. On the other hand, the three node element, which is not very accurate, is useful for educational purposes due to its simple and straightforward formulation steps.

References

Akbaş, Ş.D. (2014), "Wave propagation analysis of edge cracked circular beams under impact force", *PloS One*, **9**(6), e100496.

Akbas, S.D. (2015a), "Large deflection analysis of edge cracked simple supported beams", *Struct. Eng. Mech.*, **54**(3), 433-451.

Akbaş, Ş.D. (2015b), "On post-buckling behavior of edge cracked functionally graded beams under axial loads", *Int. J. Struct. Stab. Dyn.*, **15**(04), 1450065.

Akbaş, Ş.D. (2016a), "Post-buckling analysis of edge cracked columns under axial compression loads", *Int. J. Appl. Mech.*, **8**(8), 1650086.

Akbas, S.D. (2016b), "Analytical solutions for static bending of edge cracked micro beams", *Struct. Eng. Mech*., **59**(3), 579-599.

Aliabadi, M.H. and Rooke, D.P. (1991), "The boundary element method", *Numer. Fract. Mech.*, 90-139.

Alwar, R.S. and Nambissan, K.N. (1983), "Three-dimensional finite element analysis of cracked thick plates in bending", *Int. J. Numer. Meth. Eng.*, **19**(2), 293-303.

Atluri, S.N., Kobayashi, A.S. and Nakagaki, M. (1975), "An assumed displacement hybrid finite element model for linear fracture mechanics", *Int. J. Fract.*, **11**(2), 257-271.

Banks-Sills, L. and Bortman, Y. (1984), "Reappraisal of the quarter-point quadrilateral element in linear elastic fracture mechanics", *Int. J. Fract.*, **25**(3), 169-180.

Banks-Sills, L. and Sherman, D. (1989), "On quarter-point three-dimensional finite elements in linear elastic fracture mechanics", *Int. J. Fract.*, **41**(3), 177-196.

Barsoum, R.S. (1976), "On the use of isoparametric finite elements in linear fracture mechanics", *Int. J. Numer. Meth. Eng.*, **10**(1), 25-37.

Behera, S., Sahu, S.K. and Asha, A.V. (2015), "Vibration analysis of laminated composite beam with transverse cracks", *Adv. Struct. Eng.*, 67-75.

Belytschko, T., Lu, Y.Y. and Gu, L. (1995), "Crack propagation by element-free Galerkin methods", *Eng. Fract. Mech.*, **51**(2), 295-315.

Bordas, S.P., Rabczuk, T., Hung, N.X., Nguyen, V.P., Natarajan, S., Bog, T. and Hiep, N.V. (2010), "Strain smoothing in FEM and XFEM", *Comput. Struct.*, **88**(23), 1419-1443.

Bouboulas, A.S. and Anifantis, N.K. (2008), "Formulation of cracked beam element for analysis of fractured skeletal structures", *Eng. Struct.*, **30**(4), 894-901.

Christides, S. and Barr, A.D S. (1984), "One-dimensional theory of cracked Bernoulli-Euler beams", *Int. J. Mech. Sci.*, **26**(11-12), 639-648.

De Luycker, E., Benson, D.J., Belytschko, T., Bazilevs, Y. and Hsu, M.C. (2011), "X-FEM in isogeometric analysis for linear fracture mechanics", *Int. J. Numer. Meth. Eng.*, **87**(6), 541-565.

Dolbow, J.O., Moes, H.N. and Belytschko, T. (1999), "A finite element method for crack growth without remeshing", *Int. J. Numer. Meth. Eng.*, **46**(1), 131-150.

Duflot, M. and Nguyen-Dang, H. (2004), "A meshless method with enriched weight functions for fatigue crack growth", *Int. J. Numer. Meth. Eng.*, **59**(14), 1945-1961.

Fan, Y. and Wang, H. (2015), "Nonlinear vibration of matrix cracked laminated beams containing carbon nanotube reinforced composite layers in thermal environments", *Compos. Struct.*, **124**, 35-43.

Fett, T. and Munz, D. (1997), *Stress Intensity Factors and Weight Functions*, Vol. 1, Computational Mechanics.

Formica, G. and Milicchio, F. (2016), "Crack growth propagation using standard FEM", *Eng. Fract. Mech.*, **165**, 1-18.

Gray, L.J., Phan, A.V., Paulino, G.H. and Kaplan, T. (2003), "Improved quarter-point crack tip element", *Eng. Fract. Mech.*, **70**(2), 269-283.

Guinea, G.V., Pastor, J.Y., Planas, J. and Elices, M. (1998), "Stress intensity factor, compliance and CMOD for a general three-point-bend beam", *Int. J. Fract.*, **89**(2), 103-116.

Henshell, R.D. and Shaw, K.G. (1975), "Crack tip finite elements are unnecessary", *Int. J. Numer. Meth. Eng.*, **9**(3), 495-507.

Hussain, M.A., Coffin, L.F. and Zaleski, K.A. (1981), "Three dimensional singular element", *Comput. Struct.*, **13**(5-6), 595-599.

Ibrahim, A.M., Ozturk, H. and Sabuncu, M. (2013), "Vibration analysis of cracked frame structures", *Struct. Eng. Mech.*, **45**(1), 33-52.

Kisa, M. (2012), "Vibration and stability of axially loaded cracked beams", *Struct. Eng. Mech.*, **44**(3), 305-323.

Kisa, M. and Brandon, J. (2000), "The effects of closure of cracks on the dynamics of a cracked cantilever beam", *J. Sound Vib.*, **238**(1), 1-18.

Kisa, M., Brandon, J. and Topcu, M. (1998), "Free vibration analysis of cracked beams by a combination of finite elements and component mode synthesis methods", *Comput. Struct.*, **67**(4), 215-223.

Krawczuk, M. (1993), "A rectangular plate finite element with an open crack", *Comput. Struct.*, **46**(3), 487-493.

Lin, K.Y. and Mar, J.W. (1976), "Finite element analysis of stress intensity factors for cracks at a bi-material interface", *Int. J. Fract.*, **12**(4), 521-531.

Liu, Y. and Shu, D.W. (2015), "Effects of edge crack on the vibration characteristics of delaminated beams", *Struct. Eng. Mech.*, **53**(4), 767-780.

Ma, F.J. and Kwan, A.K.H. (2015), "Crack width analysis of reinforced concrete members under flexure by finite element method and crack queuing algorithm", *Eng. Struct.*, **105**, 209-219.

Manu, C. (1983), "Quarter-point elements for curved crack fronts", *Comput. Struct.*, **17**(2), 227-231.

Mi, Y. and Aliabadi, M.H. (1992), "Dual boundary element method for three-dimensional fracture mechanics analysis", *Eng. Anal. Bound. Elem.*, **10**(2), 161-171.

Millwater, H., Wagner, D., Baines, A., & Montoya, A. (2016), "A virtual crack extension method to compute energy release rates using a complex variable finite element method", *Eng. Fract. Mech.*, **162**, 95-111.

Nguyen-Xuan, H., Liu, G.R., Bordas, S., Natarajan, S. and Rabczuk, T. (2013), "An adaptive singular ES-FEM for mechanics problems with singular field of arbitrary order", *Comput. Meth. Appl. Mech. Eng.*, **253**, 252-273.

Nguyen-Xuan, H., Liu, G.R., Nourbakhshnia, N. and Chen, L. (2012), "A novel singular ES-FEM for crack growth simulation", *Eng. Fract. Mech.*, **84**, 41-66.

Okamura, H., Watanabe, K. and Takano, T. (1973), "Applications of the compliance concept in fracture mechanics", *Progress in Flaw Growth and Fracture Toughness Testing*, ASTM International.

Pian, T.H.H. and Moriya, K. (1978), "Three-dimensional fracture analysis by assumed stress hybrid elements", *Numer. Meth. Fract. Mech.*, 363-373.

Pian, T.H.H., Tong, P. and Luk, C.H. (1971), *Elastic Crack Analysis by a Finite Element Hybrid Method*, Massachusetts Inst. of Tech. Cambridge.

Rezaiee-Pajand, M. and Gharaei-Moghaddam, N. (2017), "A cracked element based on the compliance concept", *Theor. Appl. Fract. Mech.*, **92**, 122-132.

Rezaiee-Pajand, M. and Mousavi, R., (2009), "Formulating a Triangular element with elasto-plastic crack", *J. Civil Environ. Eng., Ferdowsi Univ. Mashhad*, **1**, 1-14. (in Persian)

Saavedra, P.N. and Cuitino, L.A. (2001), "Crack detection and vibration behavior of cracked beams", *Comput. Struct.*, **79**(16), 1451-1459.

Salah, B., Hamoudi, B., Noureddine, B. and Mohamed, G. (2014),

"Energy release rate for kinking crack using mixed finite element", *Struct. Eng. Mech.*, **50**(5), 665-677.
Schnack, E. and Wolf, M. (1978), "Application of displacement and hybrid strees methods to plane notch and crack problems", *Int. J. Numer. Meth. Eng.*, **12**(6), 963-975.
Shen, M.H. and Pierre, C. (1990), "Natural modes of Bernoulli-Euler beams with symmetric cracks", *J. Sound Vib.*, **138**(1), 115-134.
Skrinar, M. (2013), "Computational analysis of multi-stepped beams and beams with linearly-varying heights implementing closed-form finite element formulation for multi-cracked beam elements", *Int. J. Solid. Struct.*, **50**(14), 2527-2541.
Tong, P., Pian, T.H.H. and Lasry, S.J. (1973), "A hybrid-element approach to crack problems in plane elasticity", *Int. J. Numer. Meth. Eng.*, **7**(3), 297-308.
Ventura, G., Gracie, R. and Belytschko, T. (2009), "Fast integration and weight function blending in the extended finite element method", *Int. J. Numer. Meth. Eng.*, **77**(1), 1-29.
Verhoosel, C.V., Scott, M.A., De Borst, R. and Hughes, T.J. (2011), "An isogeometric approach to cohesive zone modeling", *Int. J. Numer. Meth. Eng.*, **87**(1-5), 336-360.
Viola, E., Nobile, L. and Federici, L. (2002), "Formulation of cracked beam element for structural analysis", *J. Eng. Mech.*, **128**(2), 220-230.
Yaylaci, M. (2016), "The investigation crack problem through numerical analysis", *Struct. Eng. Mech.*, **57**(6), 1143-1156.
Zeng, J., Ma, H., Zhang, W. and Wen, B. (2017), "Dynamic characteristic analysis of cracked cantilever beams under different crack types", *Eng. Fail. Anal.*, **74**, 80-94.

CC